ARMY RESEARCH LABORATORY

Characterization and Potential Application of Next Generation Commercial Surface Enhanced Raman Scattering Substrates

by Mikella E. Hankus, Ellen L. Holthoff, Dimitra N. Stratis-Cullum, and Paul M. Pellegrino

ARL-TR-5833 November 2011

NOTICES

Disclaimers

The findings in this report are not to be construed as an official Department of the Army position unless so designated by other authorized documents.

Citation of manufacturer's or trade names does not constitute an official endorsement or approval of the use thereof.

Destroy this report when it is no longer needed. Do not return it to the originator.

Army Research Laboratory
Adelphi, MD 20783-1197

ARL-TR-5833 **November 2011**

Characterization and Potential Application of Next Generation Commercial Surface Enhanced Raman Scattering Substrates

Mikella E. Hankus, Ellen L. Holthoff, Dimitra N. Stratis-Cullum, and Paul M. Pellegrino
Sensors and Electron Devices Directorate, ARL

REPORT DOCUMENTATION PAGE	Form Approved OMB No. 0704-0188

1. REPORT DATE *(DD-MM-YYYY)*	2. REPORT TYPE	3. DATES COVERED (From - To)
November 2011	Final	2010 to 2011

4. TITLE AND SUBTITLE
Characterization and Potential Application of Next Generation Commercial Surface Enhanced Raman Scattering Substrates

5a. CONTRACT NUMBER

5b. GRANT NUMBER

5c. PROGRAM ELEMENT NUMBER

6. AUTHOR(S)
Mikella E. Hankus, Ellen L. Holthoff, Dimitra N. Stratis-Cullum, and Paul M. Pellegrino

5d. PROJECT NUMBER

5e. TASK NUMBER

5f. WORK UNIT NUMBER

7. PERFORMING ORGANIZATION NAME(S) AND ADDRESS(ES)
U.S. Army Research Laboratory
RDRL-SEE-O
2800 Powder Mill Road
Adelphi MD 20783-1197

8. PERFORMING ORGANIZATION REPORT NUMBER
ARL-TR-5833

9. SPONSORING/MONITORING AGENCY NAME(S) AND ADDRESS(ES)

10. SPONSOR/MONITOR'S ACRONYM(S)

11. SPONSOR/MONITOR'S REPORT NUMBER(S)

12. DISTRIBUTION/AVAILABILITY STATEMENT
Approved for public release; distribution unlimited.

13. SUPPLEMENTARY NOTES

14. ABSTRACT

The development of a sensing platform capable of detecting and identifying hazards, including biological, chemical, and energetic platforms, is a long sought-after goal of the Army and first responder communities. Surface-enhanced Raman scatting (SERS) is a spectroscopic technique gaining popularity as a solution to many sensing needs due to its numerous advantages such as high sensitivity, little to no sample preparation required, and use in numerous environmental settings. Despite all the advantages of SERS, it still remains a marginalized sensing technique primarily due to the challenges in fabricating a reliable, highly sensitive and reproducible nanoscale surface. In this work, we show that many of these challenges have been overcome with a newly developed commercially available Klarite SERS substrate. These substrates are fabricated in a fashion similar to standard Klarite substrates, but due to changes in size and spacing of the inverted pyramidal structure there is an overall increase of SERS sensing capabilities of up to 4 orders of magnitude. In this technical report, the next-generation Klarite (308 and 309) substrates are characterized, analyte sensitivity at both 633 nm and 785 nm is demonstrated, and preliminary and non-optimized efforts with biological and energetic sensing capabilities are presented.

15. SUBJECT TERMS
Surface enhanced Raman scattering, Raman, SERS, substrate, biological, energetic, hazard, Klarite, substrate

16. SECURITY CLASSIFICATION OF:			17. LIMITATION OF ABSTRACT	18. NUMBER OF PAGES	19a. NAME OF RESPONSIBLE PERSON
a. REPORT	b. ABSTRACT	c. THIS PAGE			Mikella E. Hankus
UNCLASSIFIED	UNCLASSIFIED	UNCLASSIFIED	UU	30	19b. TELEPHONE NUMBER (*Include area code*) (301) 394-0948

Contents

List of Figures

List of Tables

Acknowledgments

Thank you, Renishaw Diagnostics, for multiple discussions regarding the response of the next generation Klarite substrates, and for the opportunity to evaluate a new product line.

1. Introduction

The development and widespread use of sensing platforms for dynamic real-time detection of hazardous materials (i.e., chemical, biological, and energetic in nature) is a perpetual goal in numerous fields of research. The ideal sensor can be used in a host of different environments; is sensitive to several types of target analytes at low concentrations; can be used in a quantitative manner; is cost efficient, small, and requires little to no sample preparation; and is commercially available. To both the U. S. Army and first responders, such an ideal sensor would be advantageous, allowing for the rapid detection and identification of hazardous materials before or after exposure to human populations. To answer this need, several sensing methodologies (for research and commercial use) have been proposed and developed. Some of the more common and effective hazard sensing technologies are based on vibrational spectroscopy like Raman and Raman-based techniques. In the sensing community, one Raman-based technique gaining particular interest is surface-enhanced Raman scattering (SERS).

Vibrational-based spectroscopic techniques like Raman rely on specific vibrations in a molecule from which a fingerprint spectrum can be generated for qualitative and quantitative measurements. Raman and Raman-based techniques are particularly well-suited for the identification and characterization of unknown targets, both hazardous and benign (*1–6*). Raman is particularly advantageous, as it (i) does not suffer from interferences from water, (ii) requires little to no sample preparation, (iii) is robust and can be used in numerous environments, (iv) is relatively insensitive to the wavelength of excitation employed, and (v) produces a narrow-band spectral signature unique to the molecular vibrations of the analyte. All of these advantages contribute to Raman spectroscopy's capability to perform sample characterization, identification, and quantification. Despite such advantages, however, Raman spectroscopy has remained a marginalized technique for trace detection of hazardous materials in the field, mainly due to the extremely low scattering cross-sections characteristic to many hazards.

SERS is a technique that overcomes the shortcomings of spontaneous Raman by greatly enhancing Raman scattering, which has been reported to detect a single molecule under ideal conditions (*7–9*). Compared to conventional Raman, the SERS enhancement has been reported to be as much as 14 orders of magnitude greater (*9*), although it is most commonly observed on the order of 7 to 8 orders of magnitude. The SERS phenomenon observed is mainly attributed to two main mechanisms: (i) the electromagnetic fields generated at or near nanostructured surfaces, and (ii) the physical or chemical adsorption of the analyte to a surface. SERS has already been shown to be a viable sensing technique for chemical, biological, and energetic hazard detection (*6, 10–15*), and has the potential to serve as a universal rapid screening tool for many types of hazardous materials.

Despite the many advantages of SERS, its application to real-world situations has remained challenging mainly due to the difficulties in fabricating highly sensitive and spectrally/physically reproducible SERS substrates; figure 1 contains example types of SERS substrates analyzed by the U.S. Army Research Laboratory (ARL). Specifically, SERS challenges are in fabricating a reproducible and a uniformly roughened nanoscale substrate from which repeatable SERS signal measurements can be collected. Several SERS platforms have been fabricated (colloids, film over nanospheres, fiber optic bundles, nanoparticles, lithographically produced structures) and demonstrated in literature. At best, some of these substrate platforms generally have 15% relative standard deviation (RSD)—the measure of the reproducibility of an analysis—from substrate-to-substrate and SERS signal enhancements of 7 to 8 orders of magnitude (*16, 17*). Consequently, many research groups and companies have focused concerted efforts toward increasing the enhancement ability, reproducibility, and mass production manufacturing of substrates. For the Army and first responders, such a substrate platform with increased sensitivity and reliability would be very advantageous.

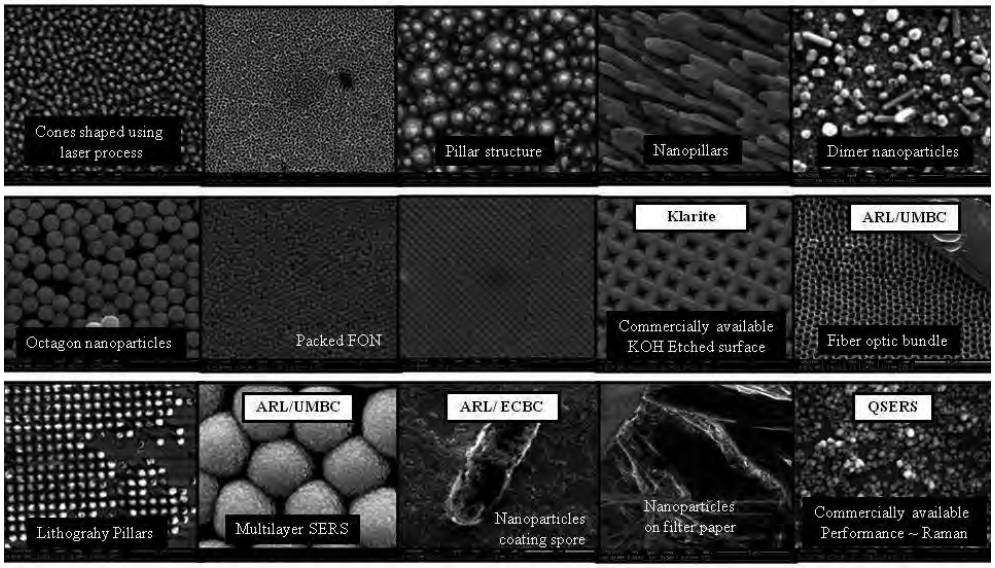

Figure 1. Several examples of SERS substrates analyzed and characterized by ARL.

Some success fabricating and applying uniform SERS substrates has been demonstrated with commercially available Klarite™ substrates (Renishaw Diagnostics.) (*18–22*). These substrates were developed using Si-based semiconductor fabrication techniques (*22*). Klarite substrates are fabricated using a well-defined silicon fabrication technique in which a silicon diode mask is defined by optical lithography, and then potassium hydroxide (KOH) surface etched. The process results in an array of highly reproducible inverted pyramid structures (*22*). These array pyramids are reported to have "hot spots" or "trapped plasmons" located inside the wells (*22*). In figure 2, a schematic of a theorized hot spot model is shown from a side view (A) and top down approach (B) (*10, 20, 22, 23*). In figure 2, hot spots (graphic not drawn to scale) are theorized to be located at the bottom of the inverted pyramid wells, as well as at the sharp

intersections of the inverted pyramid base (*10, 20, 22, 23*). These substrates have been previously characterized by our group using atomic force microscopy (AFM) analysis and plasmon data collection. From our previous work (*24*), AFM images have been used to characterize inverted pyramids estimated to be about 1.47 µm in width and 1 µm in depth. These substrates have plasmon absorbance bands located at 577 nm and 749 nm, thus demonstrating the usefulness of this substrate for a range of excitation sources. Additionally, due to the fabrication process used, under ideal conditions these substrates have demonstrated typical RSDs ranging from 10–15% under drop and dry conditions.

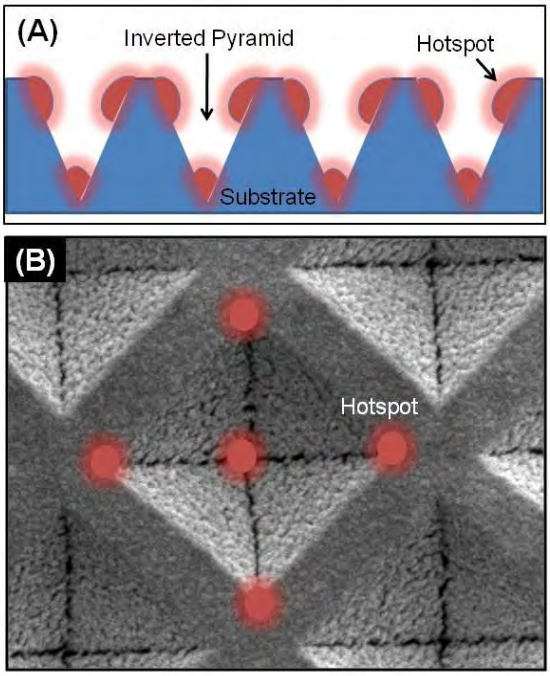

Figure 2. Schematic graphic demonstrating location of hotspots across a typical Klarite surface. In (a), a cartoon rendering displays hot spots as being located at the bottom of the inverted pyramids and at the sides. In (b), and top down SEM image with theorized hot spot location displayed as dots.

While these standard Klarite substrates do demonstrate a high degree of substrate reproducibility and very low substrate background (SERS signal and surface morphology), for many applications to real-world situations, increased analyte sensitivity is still necessary. Recently, newer prototype Klarite-based substrates have been modeled and fabricated by D3 Technologies to expand substrate capabilities. The morphologies of these substrates dramatically differ in overall shape, pitch, and spacing as compared to the standard Klarite substrate, resulting in very interesting sensing capabilities.

In this technical report, we will report on the characterization of reproducibility and limit of detection results determined with the next generation Klarite SERS substrates, using trans-1,2-bi-

(4-pyridyl) ethylene (BPE) measured at two different wavelengths 633 nm and 785 nm in a Renishaw Raman Microscope. Additionally, some preliminary biological data on spore detection and a brief effort toward hazard detection will be demonstrated with the next-generation substrates.

2. Experimental

2.1 Substrates

Commercially available slide-mounted Klarite™ 302 SERS substrates were purchased from Renishaw Diagnostics. Slides were individually wrapped and vacuum-sealed. The SERS active area on these slides is a small 4 mm × 4 mm wafer with a gold surface. The standard Klarite™ slides were only used once and opened just prior to measurement to reduce any possible surface fouling. Additionally, the substrate was submerged in ethanol to remove any possible contamination that may have accumulated on the surface. Next-generation Klarite substrates (designated as 308s and 309s) were used as received from Renishaw Diagnostics following the same procedures used for the standard substrates. Due to a limited number of substrates available, data were collected using a standard addition method. Typically, in SERS data collection on the standard and 308 substrates, five measurements across the substrate surface were collected. The next-generation 309 substrate is composed of four distinct quadrants, and due to the limited active surface area on the 309s, only two measurements were collected per quadrant. Most data in these proceedings will be presented as an average of a collected data set and the standard deviation error shown, unless otherwise indicated.

2.2 Instrumentation

Plasmon data: Plasmon data was obtained using an Avantes system. The system is controlled using AvantesSpec software. Data analysis is performed using Igor Pro 4.0 (WaveMetrics, Inc.). Unless otherwise indicated, data acquisition parameters were 500 ms exposure time, for 10 accumulations, and three averages. Using this methodology, a total of five spectra were collected from each substrate.

SEM Data: Scanning electron microscope (SEM) images was obtained using a FEI environmental SEM (Quanta 200 FEG).

Raman and SERS data: A Renishaw in Via Reflex Raman microscope was used for SERS and Raman spectra collection. Spectra were collected using the NIR 785 nm laser. The laser light was focused onto the sample using a 5X objective, exposures were 10 s in length, and three accumulations were collected per spot. Approximately 7 mW of power irradiated the surface of the substrate. Five spectra were collected from each substrate. Samples were positioned using a motorized XYZ translational stage internal to the microscope. Spectra were collected, and the

instrument was run using Wire 3.2 software operating on a dedicated computer. Data analysis was achieved using IgorPro 6.0 software (Wavemetrics) (*10*).

AFM data: All atomic force microscopy (AFM) data was obtained using a Veeco AFM. The AFM was operated in tapping mode using two tips—the OTESPA Veeco (frequency 300 kHz, length 110–180 μm), and the TAP 150Al-G Budget Sensor (soft tapping mode, resonant frequency 150 KHz).

Energetic Materials Jetted: The energetic material ammonium nitrate (AN) was selected as a target material due to its army relevance. Ammonium nitrate is commonly used in agricultural fertilizers and to produce improvised explosive devices (IEDs) in theatre. Material was printed onto the Klarite substrates using a JetLab® 4 (MicroFab Technologies). This instrument is a drop-on-demand (DOD) inkjet printing system with drop ejection drive electronics (JetDrive™ III), pressure control, a drop visualization system, and precision *X*, *Y*, *Z* motion control. The dispensing device (print head assembly, MJ-AL-01-060) consists of a glass capillary tube with a 60 μm diameter orifice coupled to a piezoelectric element and has been previously characterized by our lab (*25*).

2.3 Chemicals

All chemicals were used as received without further purification. Chemicals used included trans-1,2-bi-(4-pyridyl) ethylene (BPE) and ethanol (EtOH). The SERS response test protocol used a modified standard addition methodology developed (in partnership with Edgewood Chemical Biological Center) and commonly used for SERS DARPA evaluation program. Briefly, in these experiments the substrate was soaked in 5 mL of a BPE/EtOH solution for 10 min to insure complete binding of the BPE with the surface, and then the SERS spectra of the substrate were collected from five different points across the substrate (while still in solution). Once the measurements were collected, the old solution was removed and the substrate was soaked in the next concentration of BPE/EtOH solution. Following this protocol, typical BPE solution concentration additions included: Blank none, EtOH, $1x10^{-14}$, $1x10^{-13}$, $1x10^{-12}$, $1x10^{-11}$, $1x10^{-10}$, $5x10^{-10}$, $1x10^{-09}$, $5\ x10^{-09}$, $7.5\ x\ 10^{-09}$, $1\ x10^{-08}$, $2.5\ x\ 10^{-08}$, $5\ x10^{-08}$, $7.5\ x\ 10^{-08}$, $1\ x10^{-07}$, $2.5\ x\ 10^{-07}$, $5\ x10^{-07}$, $7.5\ x\ 10^{-07}$, and $1\ x10^{-06}$ M BPE, for a total of 20 measurements. Additionally, ammonium nitrate (AN), methanol, distilled water, and acetonitrile were obtained from Sigma-Aldrich for energetic testing.

2.4 Biological Samples

Spore suspension *B. coagulans (ATCC SUS-CG)* was purchased from Raven Biologicals and used at a log 4 or 6 population per 0.1 mL of solution. For experiments in this report, a 1 μL aliquot of spore suspension was drop-dried onto the active area of the Klarite substrate. Once the suspension had completely dried, SERS measurements were collected. Due to the nature of the drop dry technique (*24*), uneven coverage of the spore samples did occur with a higher concentration being located around the "edge" of the coffee ring. To compensate for this,

multiple measurements were collected towards the "center" of each analyte ring on the substrate surface (*6*).

3. Results and Discussion

3.1 Physical Characterization

Standard Klarite and next-generation Klarite substrates were first physically characterized by SEM image analysis and then AFM. In figure 3, a visual schematic of a standard Klarite and next-generation Klarite substrates is shown in an effort to demonstrate parameters measured for characterization. In figure 3a, a cartoon graphic of a typical Klarite substrate is demonstrated with the Klarite chip active area shown. Figure 3b includes a description of AFM data for the substrate with inverted pyramids clearly shown; (a) is the length of a pyramid, (b) is the height of a pyramid, (c) is the spacing between the inverted pyramids, and (d) is the length of the pyramid wall. In figure 3c, the sensing area for the three different types of substrate is shown. Klarite 302 and 308 are both composed of a single uniform sensing area, while Klarite 309 consists of four different quadrants. In figure 3d, a modified SEM image demonstrates the different measurements on the substrate, inner (active, in black marks) and outer (overall area, in white marks) portion of an inverted pyramid, (a) length of pyramid, and (b) spacing between pyramids. All of these measurements are used for determination of the standard sensing area per inverted pyramid (calculation accounts for pyramid structure) and the overall percentage of active sensing area per chip. Surface calculations are used to draw conclusions and explain possible trending.

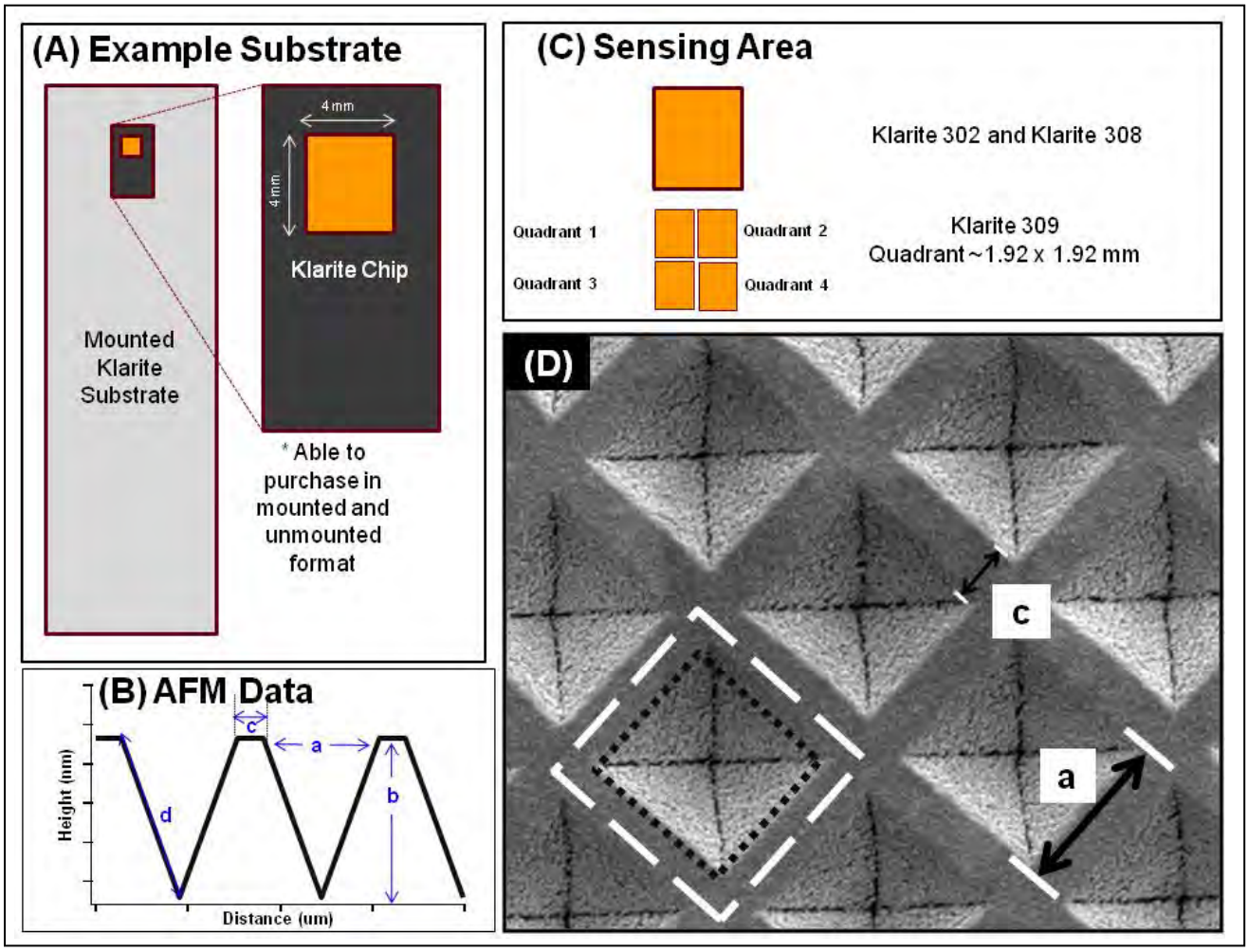

Figure 3. A visual schematic of standard Klarite and next generation Klarite substrates is shown. In (a), a cartoon of a typical Klarite substrate is demonstrated with the Klarite chip demonstrated for clarity. In (b) AFM data for the substrate with inverted pyramids is clearly shown, (a) is the length of a pyramid, (b) is the height of a pyramid, (c) is the spacing between the inverted pyramids, and (d) is the length of the pyramid wall.

NOTE: In figure 3(c) the sensing area for the three different types of substrate is shown. Klarite 302 and 308 are both composed of a single uniform sensing area, while Klarite 309 consists of four different quadrants. In figure 3(d), a modified SEM image demonstrates the different measurements on the substrate, inner (active, in black marks) and outer (overall area, in white marks) portion of an inverted pyramid, (a) length of pyramid, and (b) spacing between pyramids.

To establish the total number of cells (inverted pyramids + ½ the distance between the neighbor cell) for the active area of the substrate and to determine the total % of the surface that was composed of cells, a combination of information from both SEM and AFM analysis was analyzed. Using SEM and AFM data analysis sizes of inverted pyramids for the different types of Klarite substrate were established; see figure 4a for an example SEM of a Klarite 309 substrate and figure 4b for AFM data. From data analysis it was determined that a standard Klarite substrate has an outer width of about 2040 nm, and an inner pyramid width of 1470 nm, for a total sensing area of 51.9% of a single pyramid. Assuming an overall active chip size of

4 mm x 4 mm, the total number of cells for each 302 substrate is around 3.84 x 10^6. The Klarite 308 substrate has an outer width of 636.4 nm, and an inner pyramid width of about 454.0 nm, for a total sensing area of 50.9% of a single pyramid. Assuming an overall active chip size of 4 mm x 4 mm, the total number of cells for each 308 substrate is around 3.95 x 10^7. The Klarite 309 Quadrant 1 substrate has an outer width of about 758.1 nm, and an inner pyramid width of 580.0 nm, for a total sensing area of 66.7%. Assuming an overall active chip size of 1.92 mm x 1.92 mm, the total number of cells for each substrate is around 6.41 x 10^6. The Klarite 309 Quadrant 2 substrate has an outer width of about 806.5 nm, and an inner pyramid width of 484.0 nm, for a total sensing area of 43.3%. Assuming an overall active chip size of 1.92 mm x 1.92 mm, the total number of cells for each substrate is around 5.67 x 10^6. The Klarite 309 Quadrant 3 substrate has an outer width of about 790.3 nm, and an inner pyramid width of 661.0 nm, for a total sensing area of 69.5%. Assuming an overall active chip size of 1.92 mm x 1.92 mm, the total number of cells for each substrate is around 5.09 x 10^6. The Klarite 309 Quadrant 4 substrate has an outer width of about 806.5 nm, and an inner pyramid width of 564.0 nm, for a total sensing area of 62.0%. Assuming an overall active chip size of 1.92 mm x 1.92 mm, the total number of cells for each substrate is around 5.67 x 10^6. From this information it can be concluded that the next generation Klarite 308 has a significantly higher overall density of cells for the surface area as compared to the Klarite 302, and thus potentially amount of SERS hot spot area. Ranking the % of cell "active" greatest to smallest on the 309 substrate quadrant 3 is largest, followed by quadrant 1, followed by quadrant 4 and then quadrant 2 has the smallest overall % active area active. From this observed trending on the 309, it might be concluded that quadrant 3 will outperform quadrant 2.

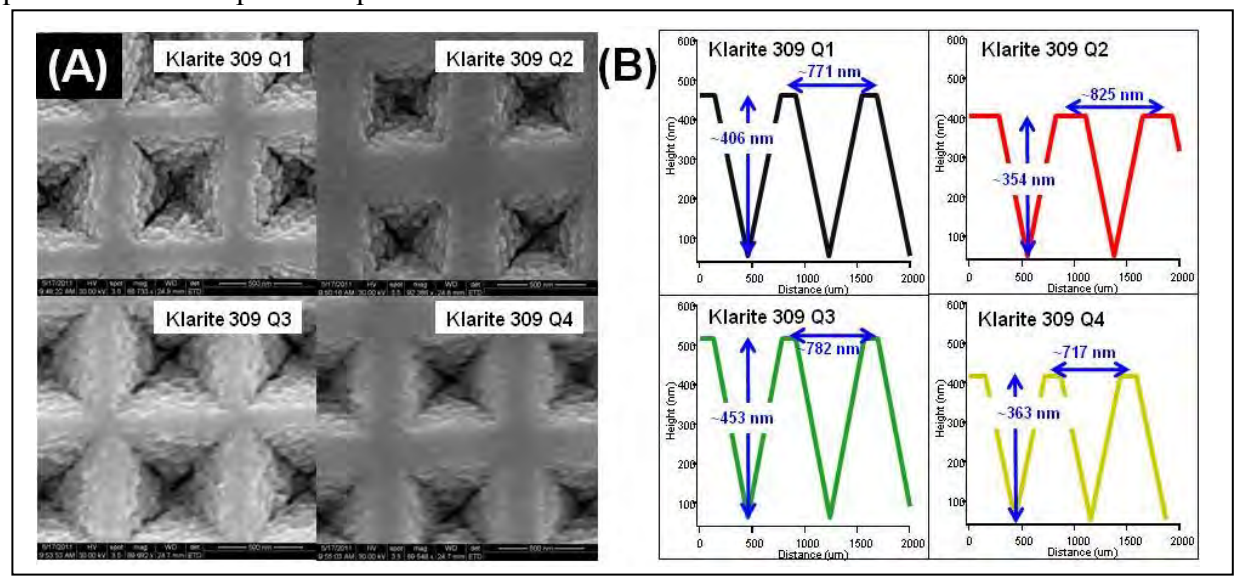

Figure 4. In (a) example SEM images of different quadrants of Klarite 309 substrate are shown. An example of typical approximate AFM data collected from each of the four quadrants of Klarite 309 is shown in (b). From this data in (b), it was determined that quadrant 1 has a depth of about 406 nm, quadrant 2 has a depth of about 354 nm, quadrant 3 has a depth of about 453 nm, and quadrant 4 has a depth of about 363 nm.

To get an overall idea about the depths of features across the surface and overall pyramid surface area, AFM analysis was used. In figure 5, next generation Klarite 308 physical characterization data is shown. In table 1, a summary of these results is provided, including the number of cells per chip area, well width and height, distance between features, slant length, pyramid surface area, and percent of cell area deemed active for the standard commercial Klarite 302, and for the prototype Klarite 308 and 309 series. Comparing the pyramid surface area between the 302 and the 308, we see that overall the 302 has a much larger surface area. However, there are significantly more "cells" for the Klarite 308 as compared to 302, and the cells are placed much more closely together which might affect overall SERS signal enhancing capabilities. The trend observed from largest to smallest overall inverted pyramid surface area and active area on the Klarite 309 is quadrant 3, quadrant 1, quadrant 4, and quadrant 2. Additionally, when comparing the different quadrants of the 309, it can be observed that ranking pyramid depth (b) from greatest to smallest, we observe the following trend: quadrant 3, quadrant 1, quadrant 4, and quadrant 2. Comparing spacing between features, smallest to greatest, we again observe the trend going from quadrant 3, quadrant 1, quadrant 4, and, finally, quadrant 2. All of these physical parameters may have a significant influence on the overall SERS activity of these different quadrants.

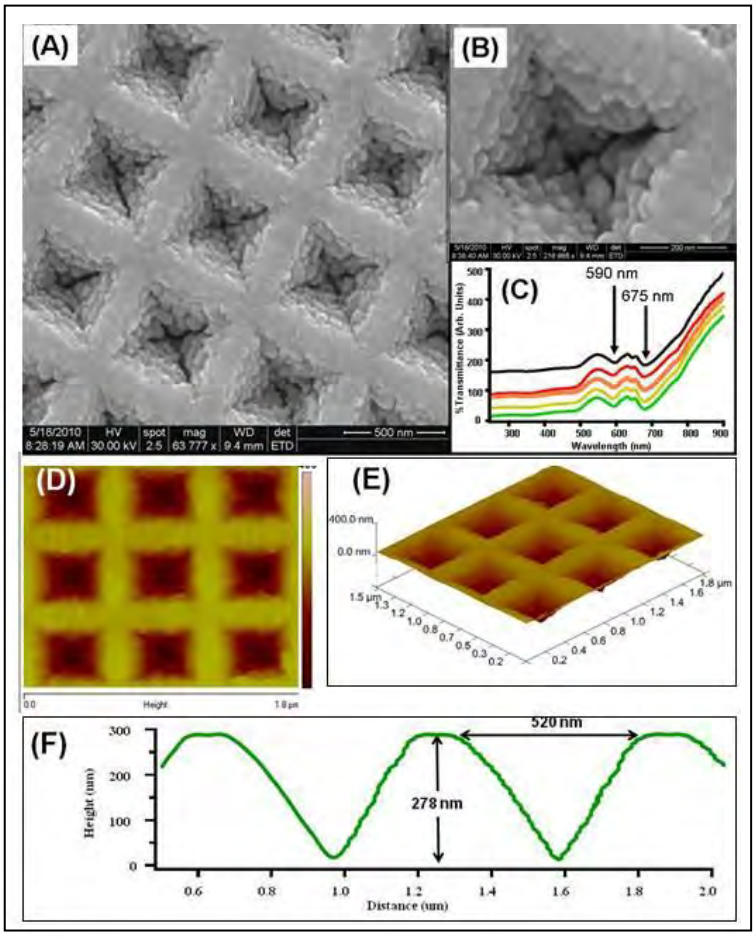

Figure 5. Next generation 308 Klarite substrate. (a) SEM image at 63,777x magnification, demonstrating spacing between wells, (b) SEM image at 216,988x magnification, showing "roughness" of single well, and (c) plasmon data demonstrating absorbance bands located at 590 nm and 675 nm. In (d-e) example AFM images of Klarite 308 substrate. In (f), AFM data demonstrates the typical depth is 278 nm and the length of pyramids is 520 nm for this substrate.

Table 1. Comparison physical parameters of standard Klarite, Klarite 308 and Klarite 309 quadrants as determined by SEM and AFM analysis.

Substrate Type	Total number of cells for chip area	(a) Well width (nm)	(b) Height well (nm)	(c) Distance between features (nm)	(d) Slant length	Pyramid surface area	% of "cell" area active
Klarite 302	3.84E+06	1470	1000	570	1428	2.43E+13	51.9%
Klarite 308	3.95E+07	454	278	200	422	2.17E+11	50.9%
Klarite 309 Q1	6.41E+06	630	406	141	514	2.57E+11	66.7%
Klarite 309 Q2	5.67E+06	543	354	282	446	1.43E+11	43.3%
Klarite 309 Q3	5.90E+06	652	453	130	558	3.09E+11	69.5%
Klarite 309 Q4	5.67E+06	565	363	152	460	1.66E+11	62.0%

3.2 Plasmon Absorbance Data

Plasmon absorbance data for the different SERS substrates were collected and the results are shown in figure 6. From these data, it should be possible to determine with substrates are most similar and draw initial conclusions on observed sensitivity trending. The plasmon bands of Klarite 302 and 308 are found to be most similar in location. The second plasmon band feature for the different quadrants of 309 ranked from greatest to lowest wavelength are: quadrant 3, quadrant 1, quadrant 4, and quadrant 2.

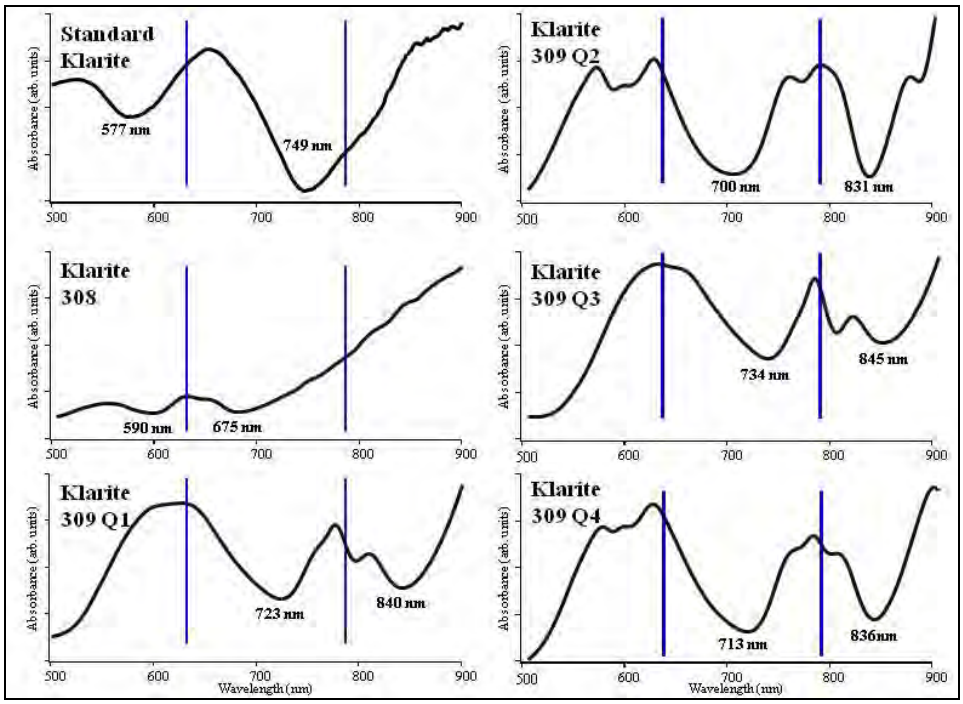

Figure 6. Plasmon data for all Klarite substrates. Lines indicate location of 633 and 785 nm lasers relative to location of plasmon absorbance bands.

3.3 Determination of Detection Capabilities

Limits of detection and overall typical signal to noise (S/N) ratios were determined following the SERS BPE testing evaluation previously described and briefly outlined in the experimental section. For these experiments, two different wavelengths were evaluated to determine if the location of the plasmon band would influence the overall SERS response of the substrates. For LOD determination, the S/N ratios and error were calculated for all substrate types over 20 different calculations and at two different wavelengths. The target analyte used was BPE (see figure 7a for an example spectrum of BPE at 785 nm in EtOH) with a 1200 cm^{-1} band clearly indicated. In figure 7b, an example S/N comparison between the Klarite 302 and 308 is clearly demonstrated. An example of data analysis is shown in figure 7c from a standard Klarite substrate, collected with 785 nm laser, averaged data points with S/N >3, error represents 1 std. dev. In this data set the R^2 value observed is 0.941. Using this type of analysis, it was possible to calculate the sensitivity for all substrate types at the two different wavelengths; see table 2 for a summary of results. It should be noted that this LOD is analyte-specific, as different chemical interactions between the surface and the analyte can occur by changing the identity of the chemical of interest. Similar data were collected and analyzed for both the 633 nm and 785 nm laser; see table 2 for a summary of LOD results.

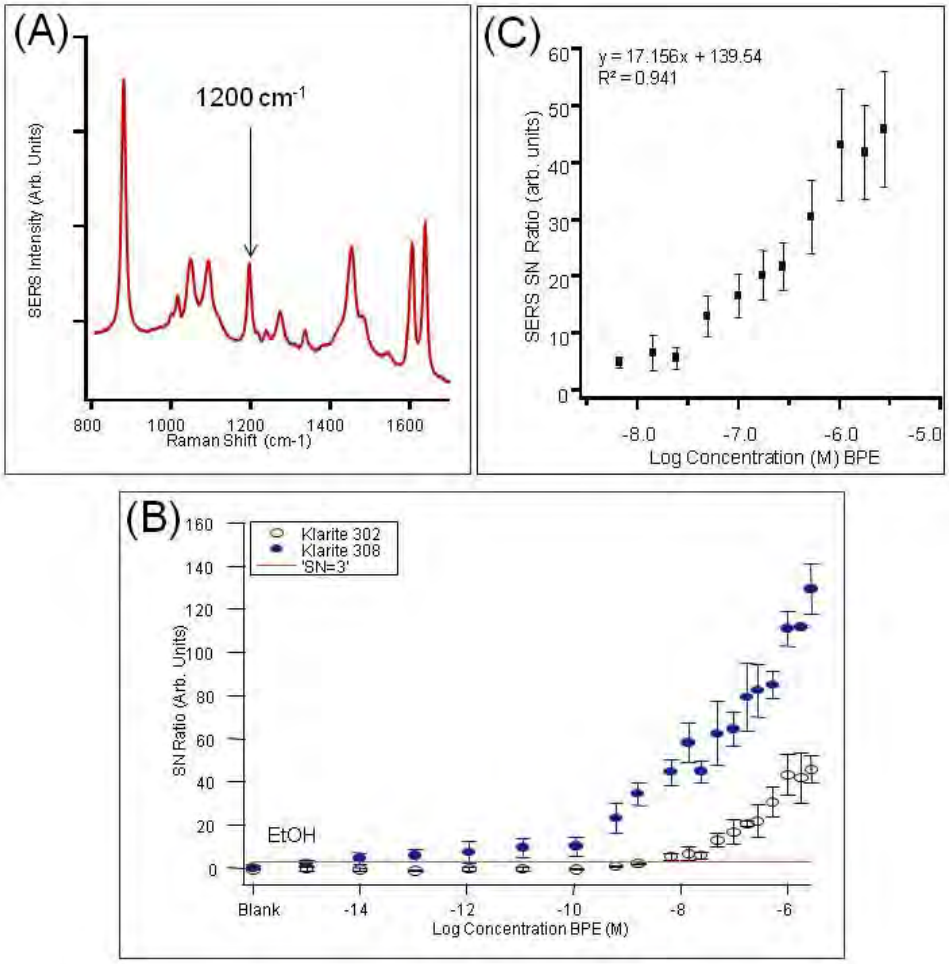

Figure 7. (a) Typical BPE spectrum shown with 1200 cm^{-1} band indicated. (b) Comparison of S/N ratio of Klarite 308 and 302. Red line indicates S/N=3. (c) Example of results from a standard Klarite substrate, collected with 785 nm laser, averaged data points with S/N >3, error represents 1 std. dev. In this data set the R^2 value observed is 0.941. Quadrant 3 (Q3) is shown to have the overall highest SERS sensing capabilities.

Table 2. Comparison of standard Klarite 302, Klarite 308 and Klarite 309 quadrants as determined by SEM analysis and sensitivity determination at 633 nm and 785 nm.

Substrate Type	Plasmon location	(number of cells) X (surface area)	Sensitivity @ 633 nm laser excitation (BPE)	Sensitivity @ 785 nm laser excitation (BPE)
Klarite 302	577, 749	9.32E+19	5.83E-09	1.99E-08
Klarite 308	590, 675	8.60E+18	6.27E-10	9.46E-13
Klarite 309 Q1	723, 840	1.59E+18	1.98E-09	5.40E-08
Klarite 309 Q2	700, 831	7.74E+17	2.88E-08	1.99E-08
Klarite 309 Q3	734, 845	1.87E+18	2.16E-09	6.89E-09
Klarite 309 Q4	713, 836	1.19E+18	1.97E-09	2.31E-08

From the results shown in table 2, it can be clearly seen that the best results were obtained using Klarite 308 with 785 nm excitation can for an overall improvement of almost four orders of magnitude in LOD for this analyte, compared to the standard Klarite 302 under the same experimental conditions. Using 633 nm laser excitation, the data shows that the Klarite 308 outperforms other substrates; however, the changes in sensing capabilities were not substantial. From the characterization data discussed (density comparison, amount of active area, location of plasmon absorbance bands) in the previous section, some trending correlates with overall SERS sensing performance observed. This implies that there might be other parameters besides those measured affecting overall SERS enhancing capabilities, and future modeling studies will be conducted.

3.4 Biological Sample Evaluation

For Army-relevant use, SERS substrates must be sensitive to chemical analytes and also be usable in a range of biological samples. Bacteria and spores are just one example of the type of sample for which rapid identification would be advantageous, specifically being able to differentiate between harmful and benign species. In theory, different species of the same type of bacteria have slight differences in their outer wall composition. As SERS is a near-field technique, spore samples coming into contact with the surface should only have the outer wall (1–2 nm from the surface) measured with SERS. Therefore, it should be possible to differentiate between different types of spore samples.

Biological samples still remain some of the more challenging analytes due to their complex natural composition, low Raman cross-sections, and extended structure, which poses unique sampling issues due to reduced contact with the entire enhancing surface. The detection capabilities of a standard Klarite and the next generation Klarite substrates were evaluated with the spore sample *B. coagulans*. In these experiments, different substrates and the changes in overall band intensity were evaluated.

For these experiments, an aliquot of the common bacillus spore *B. coagulans* was drop-dried onto the SERS substrate active surface. As the sample dried, the spores arbitrarily oriented across the surface; see figures 8a–f for examples of spore interactions with the multiple SERS substrate surfaces. As can be seen in figure 8a, the spore is sitting inside the well. In figures 8b–f, the spore sits across the SERS surface, thereby proving a significant challenge for sensing. As the spore is a rather large biological sample, its interaction with the surface is going to be limited to the areas where it comes into contact with the SERS surface.

The resulting spectra from the spore sample were collected from five different spots across the surface (figure 8g). As shown in figure 8g, the spectra all appear fairly consistent, with a main triplet band located at around 1000 cm^{-1}. For the purpose of this report, band identification is not discussed. From these results, it can be concluded that the different substrate types demonstrate similar ability to detect the sample. Additionally, there are no obvious changes in overall band intensity, suggesting that the different contact and interaction between the spore

sample and surface does not have a dramatic effect on overall SERS enhancement. It can be concluded from these results that, most likely, a more advanced solution is needed for larger biological samples.

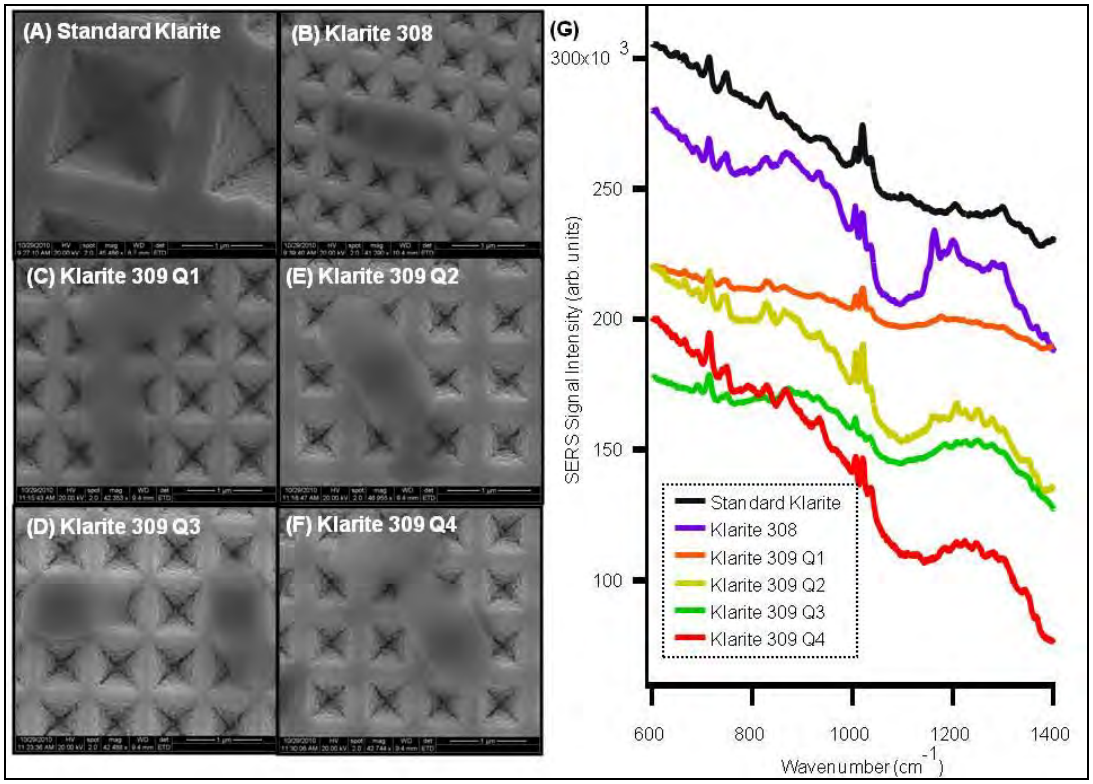

Figure 8. SEM images of spore samples on different Klarite substrate types (a–f). Notice the dramatic difference in size between the spore and the active areas on the Klarite surface. Spectra for bacillus spore *B. coagulans* on different substrate types.

3.5 Energetic Sample Evaluation

Hazard detection capabilities of the different SERS substrates, from the Army-relevant compound ammonium nitrate (AN) a common fertilizer and component of IEDs, were evaluated. The compound AN was DOD-printed onto the different SERS substrates at concentrations of 0.05 and 0.50ug/cm^2. These concentrations were selected, as they represent quantities that could be found in a typical fingerprint. SEM images of the two different concentrations deposited onto a standard Klarite 302 substrate are shown in figures 9a and b. From the SEM images, it can be clearly seen that the drops observed do vary in size. During the collection of SEM data it was observed that the drops formed tight ball shapes, and, thus, were not evenly spreading across the surface of the SERS substrate. This lack of spreading means that potentially the compound was not able to be deposited across hot spot areas on the surface, and, consequently, some amount of error spread is expected in the data. The SERS spectra for AN at 785 nm were collected from three different spots across each substrate type surface, and the band located at 1030cm^{-1} was used for analysis. For comparison purposes, spontaneous Raman signatures were also collected

from each substrate type. See figure 9C for SN ratios from different Klarite substrates at two different concentrations of AN. From these data in figure 9c, at an AN concentration of 0.05 µg/cm^2, it can be concluded that at Klarite 309 quadrant 3 and 4 outperformed Klarite 308. At a concentration of 0.50 µg/cm^2, Klarite 308 quadrant 3 and Klarite 308 perform similarly. These results were not expected, as previous studies had indicated that the Klarite 308 would most likely outperform the other Klarite substrate types using entirely solution phase measurements. It should also be noted that both next-generation substrates outperformed the standard Klarite. Based on these results, additional testing of different types of energetic samples and energetic samples in solution will be conducted.

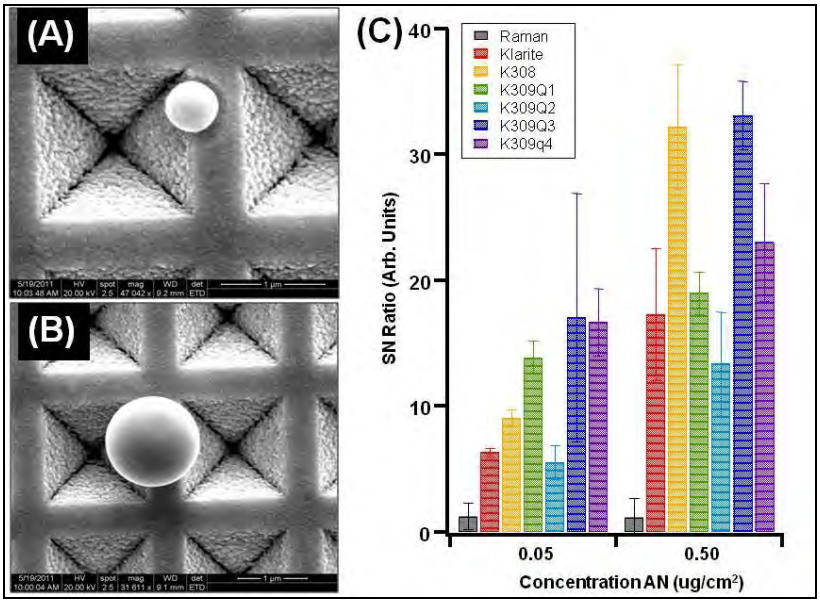

Figure 9. SEM images of AN on Klarite substrate at two different concentrations (a) 0.05 µg/cm^2, and (b) 0.50 µg/cm^2. In (c) S/N comparison at the different concentrations for the different substrates.

4. Conclusions

In this report, characterization and comparison of the next-generation Klarite substrates 308 and 309 to the standard Klarite substrate has been shown for different excitation wavelengths 633 nm and 785 nm. From the characterization results looking at a common SERS active analyte BPE, it can be concluded that overall that the next-generation Klarite substrate's SERS sensing performance is significantly better, up to four orders of magnitude in some cases as compared to the standard Klarite 302. Future work will focus on testing next-generation Klarite response to various energetic samples and modeling efforts to determine hot spot location across a substrate surface. Additionally, as these substrates are optimized and made more market-ready, we expect to re-evaluate their sensitivity and reproducibility.

5. References

1. Hankus, M. E.; Cullum, B. M. SERS Probes for the Detection and Imaging of Viochemical Apecies on the Nanoscale. *Proceedings of the SPIE - The International Society for Optical Engineering*, 638004-638001-638012 (2006).

2. Hankus, M. E.; Cullum, B. M. SERS Nanoimaging Probes for Characterizing Extracelllar Surfaces - art. no. 675908 *Smart Biomedical and Physiological Sensor Technology V* **2007**, 75908–75908.

3. Hankus, M. E.; Gibson, G.; Chandrasekharan, N.; Cullum, B. M. Surface-enhanced Raman Scattering (SERS) - nanoimaging Probes for Biological Analysis. *Smart Medical and Biomedical Sensor Technology Ii* **2004**, 106–116.

4. Hankus, M. E.; Gibson, G. J.; Cullum, B. M. Characterization and optimization of novel surface-enhanced Raman scattering (SERS)-based nanoimaging probes for chemical imaging. *Proceedings of the SPIE - The International Society for Optical Engineering*, 600704-600701-600711 (2005).

5. Hankus, M. E.; Li, H. G.; Gibson, G. J.; Cullum, B. M. Surface-enhanced Raman Scattering-based Nanoprobe for High-resolution, Non-scanning Chemical Imaging. *Analytical Chemistry* **2006**, 7535–7546.

6. Hankus, M. E.; Stratis-Cullum, D. N.; Pellegrino, P. M. Towards Advanced Biological Detection using Surface Enhanced Raman Scattering (SERS)-based Sensors. *Biosensing Iii*, **2010**.

7. Kneipp, K.; Kneipp, H. Detection, Identification, and Tracking of Biomolecules at the Single Molecule Level Using SERS. *Biophysical Society* **2005**.

8. Kneipp, K.; Kneipp, H.. Single Molecule Raman Scattering. *Appl. Spectros.* **2006**, *322A*.

9. Kneipp, K.; Kneipp, H.; Dasari, R. R.; Feld, M. S. Single Molecule Raman Spectroscopy using Silver and Gold Nanoparticles. *Indian Journal of Physics and Proceedings of the Indian Association for the Cultivation of Science-Part B* **2003**, 39–47.

10. Hankus, M. E.; Stratis-Cullum, D. N.; Pellegrino, P. M. Characterization of Next-generation Commercial Surface-enhanced Raman Scattering (SERS) Substrates. P*roc. SPIE, 80180P* (2011).

11. Holthoff, E. L.; Stratis-Cullum, D. N.; Hankus, M. E. Xerogel-Based Molecularly Imprinted Polymers for Explosives Detection. *Chemical, Biological, Radiological, Nuclear, and Explosives (Cbrne) Sensing Xi*, (2010).

12. Holthoff, E. L.; Stratis-Cullum, D. N.; Hankus, M. E. A Nanosensor for TNT Detection Based on Molecularly Imprinted Polymers and Surface Enhanced Raman Scattering. *Sensors* **2011**, 2700–2714.

13. Holthoff, E. L.; Stratis-Cullum, D. N.; Hankus, M. E.; Pellegrino, P. M. ANYL 57-Nanosensor for explosives' detection based on molecularly imprinted polymers and surface enhanced Raman scattering. Abstracts of Papers of the American Chemical Society, 57-ANYL (2009).

14. Jian, S.; Hankus, M. E.; Cullum, B. M. SERS based Immuno-microwell Arrays for Multiplexed Detection of Foodborne Pathogenic Bacteria, *Proceedings of the SPIE - The International Society for Optical Engineering*, 73130K (73110 pp.) (2009).

15. Guicheteau, J.; Argue, L.; Emge, D.; Hyre, A.; Jacobson, M.; Christesen, S. *Bacillus* Spore Classification via Surface-Enhanced Raman Spectroscopy and Principle Component Analysis. *Applied Spectroscopy* **2008**, 267–272.

16. Li, H.; Baum, C. E.; Sun, J.; Cullum, B. M.; Multilayer Enhanced SERS Active Materials: Fabrication, Characterization, and Application to Trace Chemical Detection. *SPIE* **2006**, 621804.

17. Li, H.; Patel, P. H.; Cullum, B. M. Novel Multilayered SERS Substrates for Trace Chemical and Biochemical Analysis. *SPIE* **2004**.

18. Alexander, T. A. Applications of Surface-Enhanced Raman Spectroscopy (SERS) for Biosensing: An Analysis of Reproducible, Commercially Available Substrates. *SPIE* **2005**, 600703.

19. Alexander, T. A. Development of Methodology Based on Commercialized SERS-active Susbtrates for Rapid Discrimination of Poxviridae Virions. *Anal. Chem.* **2008**, 2817–2825.

20. Alexander, T. A.; Le, D. M. Characterization of a Commercialized SERS-active Substrate and its Application to the Identification of Intact Bacillus Endospores. *Appl. Opt.* **2007**.

21. Alexander, T. A.; Pellegrino, P. M.; Gillespie, J. B. Near-Infrared Surface-Enhanced-Raman-Scattering-Mediated Detection of Single Optically Trapped Bacterial Spores. *Applied Spectroscopy* **2003**, 1340–1345.

22. Netti, M. C.; Zoorob, M. E.; Charlton, M.C.B.; Ayliffe, P.; Mahnkopf, S.; Stopford, P.;Todd, K.; Lincoln, J. R.; Perney, N.M.B.; Baumberg, J. J. Probing Molecules by Surface-Enhanced Raman Spectroscopy. *SPIE* **2006**.

23. Perney, N.M.B.; Baumberg, J. J.; Zoorob, M. E.; Charlton, M.E.B.; Mahnkopf, S.; Netti, C. M. Tuning Localized Plasmons in Nanostructured Substrates for Surface-enhanced Raman Scattering. *Optics Express* **2006**, 847–857.

24. Hankus, M.; Stratis-Cullum, D.; Pellegrino, P. *Enabling Technologies for Point and Remote Sensing of Chemical and Biological Agents Using Surface Enhanced Raman Scattering (SERS) Techniques*; ARL Technical Report, 132 (2009).

25. Holthoff, E. L.; Hankus, M. E.; Pellegrino, P. M. Investigating a Drop-on-demand Microdispenser for Standardized Sample Preparation, *Proc. SPIE - Int. Soc. Opt. Eng*, 80181F-80190F (2011).

List of Symbols, Abbreviations, and Acronyms

AFM	atomic force microscopy
AN	ammonium nitrate
ARL	U.S. Army Research Laboratory
BPE	trans-1,2-bi-(4-pyridyl) ethylene
DOD	drop-on-demand
EtOH	ethanol
IED	improvised explosive device
KOH	potassium hydroxide
RSD	relative standard deviation
SEM	Scanning electron microscope
SERS	surface-enhanced Raman scattering

NO. OF COPIES	ORGANIZATION
1 ELEC	ADMNSTR DEFNS TECHL INFO CTR ATTN DTIC OCP 8725 JOHN J KINGMAN RD STE 0944 FT BELVOIR VA 22060-6218
3 HC 3 CD 1 ELEC	PAUL PELLEGRINO U.S. ARMY RESEARCH LABORATORY RDRL-SEE-O 2800 POWDER MILL ROAD ADELPHI, MD 20783 PAUL.M.PELLEGRINO.CIV@MAIL.MIL
3 HC 1 ELEC	ELLEN HOLTHOFF U.S. ARMY RESEARCH LABORATORY RDRL-SEE-O 2800 POWDER MILL ROAD ADELPHI, MD 20783 ELLEN.L.HOLTHOFF.CIV@MAIL.MIL
3 HC 1 ELEC	MIKELLA HANKUS U.S. ARMY RESEARCH LABORATORY RDRL-SEE-O 2800 POWDER MILL ROAD ADELPHI, MD 20783 MIKELLA.E.HANKUS.CIV@MAIL.MIL
3 HC 1 ELEC	DIMITRA STRATIS-CULLUM U.S. ARMY RESEARCH LABORATORY RDRL-SEE-O 2800 POWDER MILL ROAD ADELPHI, MD 20783 DIMITRA.N.STRATIS-CULLUM.CIV@MAIL.MIL
1 ELEC	GARY WOOD U.S. ARMY RESEARCH LABORATORY RDRL-SEE 2800 POWDER MILL ROAD ADELPHI, MD 20783 GARY.L.WOOD.CIV@MAIL.MIL
1 ELEC 1HC	LINDA BLISS U.S. ARMY RESEARCH LABORATORY RDRL-SEE 2800 POWDER MILL ROAD ADELPHI, MD 20783 LINDA.A.BLISS.CIV@MAIL.MIL
3 HCS	US ARMY RSRCH LAB ATTN IMNE ALC HRR MAIL & RECORDS MGMT ATTN RDRL CIO LL TECHL LIB ATTN RDRL CIO MT TECHL PUB ADELPHI MD 20783-1197

TOTAL: 26 (7 ELEC, 16 HC, 3 CD)

INTENTIONALLY LEFT BLANK.